

1995122619

N95-29040

Experimental and Analytical Characterization of
Triaxially Braided Textile Composites

John E. Masters
Lockheed Engineering and Science

511-24

Mark J. Fedro
Boeing Defense and Space Group

512.74

Peter G. Ifju
Virginia Polytechnic Institute

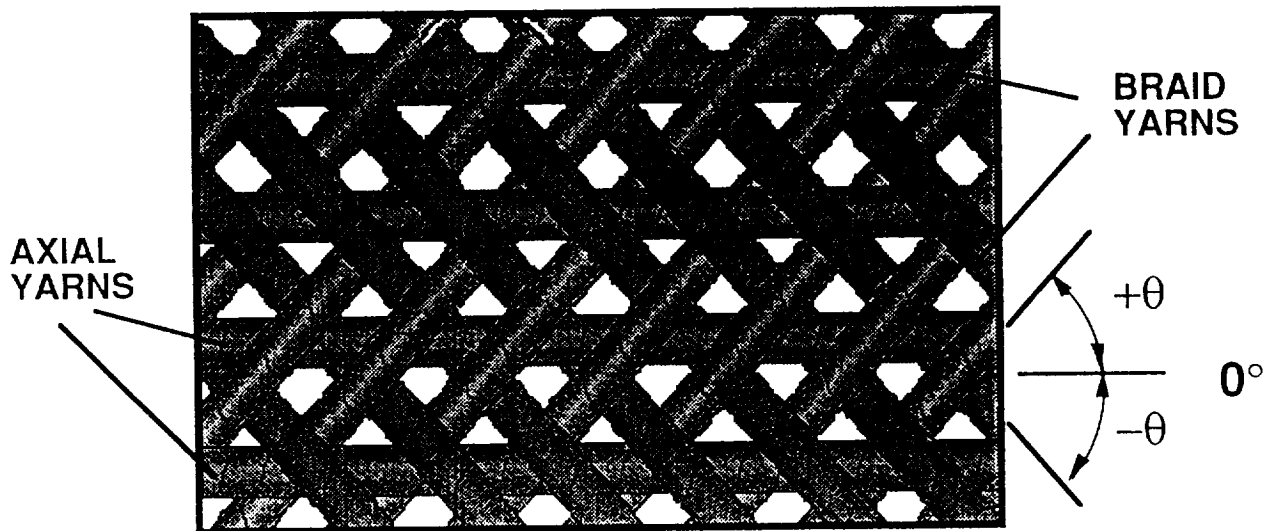
OUTLINE:

- DEFINITION OF MATERIAL
- EXPERIMENTAL RESULTS
- ANALYTICAL RESULTS
- SUMMARY

There were two components, experimental and analytical, to this investigation of triaxially braided textile composite materials. The experimental portion of the study centered on measuring the materials' longitudinal and transverse tensile moduli, Poisson's ratio, and strengths. The identification of the damage mechanisms exhibited by these materials was also a prime objective of the experimental investigation. The analytical portion of the investigation utilized the Textile Composites Analysis (TECA) model to predict modulus and strength. The analytical and experimental results were compared to assess the effectiveness of the analysis.

The figures contained in this paper reflect the presentation made at the conference. They may be divided into four sections, as the outline listed above illustrates. A definition of the material system tested is contained in the next two figures. This is followed by a series of figures summarizing the experimental results. These figures contain results of a Moire interferometry study of the strain distribution in the material, examples and descriptions of the types of damage encountered in these materials, and a summary of the measured properties. A description of the TECA model follows the experimental results. This includes a series of predicted results and a comparison with measured values. Finally, a brief summary completes the paper.

TRIAXIAL BRAID PATTERN



The specimens studied in this investigation featured 2-D triaxially braided AS4 graphite fiber preform impregnated with Shell 1895 epoxy resin. In a triaxially braided preform three yarns are intertwined to form a single layer of $0/\pm\theta$ material. In this case, the braided yarns are intertwined in a 2X2 pattern. Each $+\theta$ yarn crosses alternately over and under two $-\theta$ yarns and vice versa. The 0° yarns were inserted between the braided yarns. This yields a two dimensional material; there are no through-the-thickness fibers.

The yarns were braided over a cylindrical mandrel to a nominal thickness of .125 in. The desired preform thickness was achieved by overbraiding layers. After braiding, the preforms were removed from the mandrel, slit along the 0° fiber direction, flattened and border stitched to minimize fiber shifting. The resin was introduced via a resin transfer molding process.

TRIAxIAL BRAID CONFIGURATIONS

MATERIAL	BRAID PATTERN	BRAIDER YARN SIZE (K)	0° YARN SIZE (K)	PERCENT 0° YARNS (%)	0° YARN SPACING (YARN/IN.)	BRAID YARN SPACING (YARN/IN.)
A1	0/± 63°	12K	24K	31.5	4.17	9.16
B1	0/±66.5°	6K	18K	37.6	4.77	11.98
B2	0/±70°	6K	18K	34.0	4.37	12.74

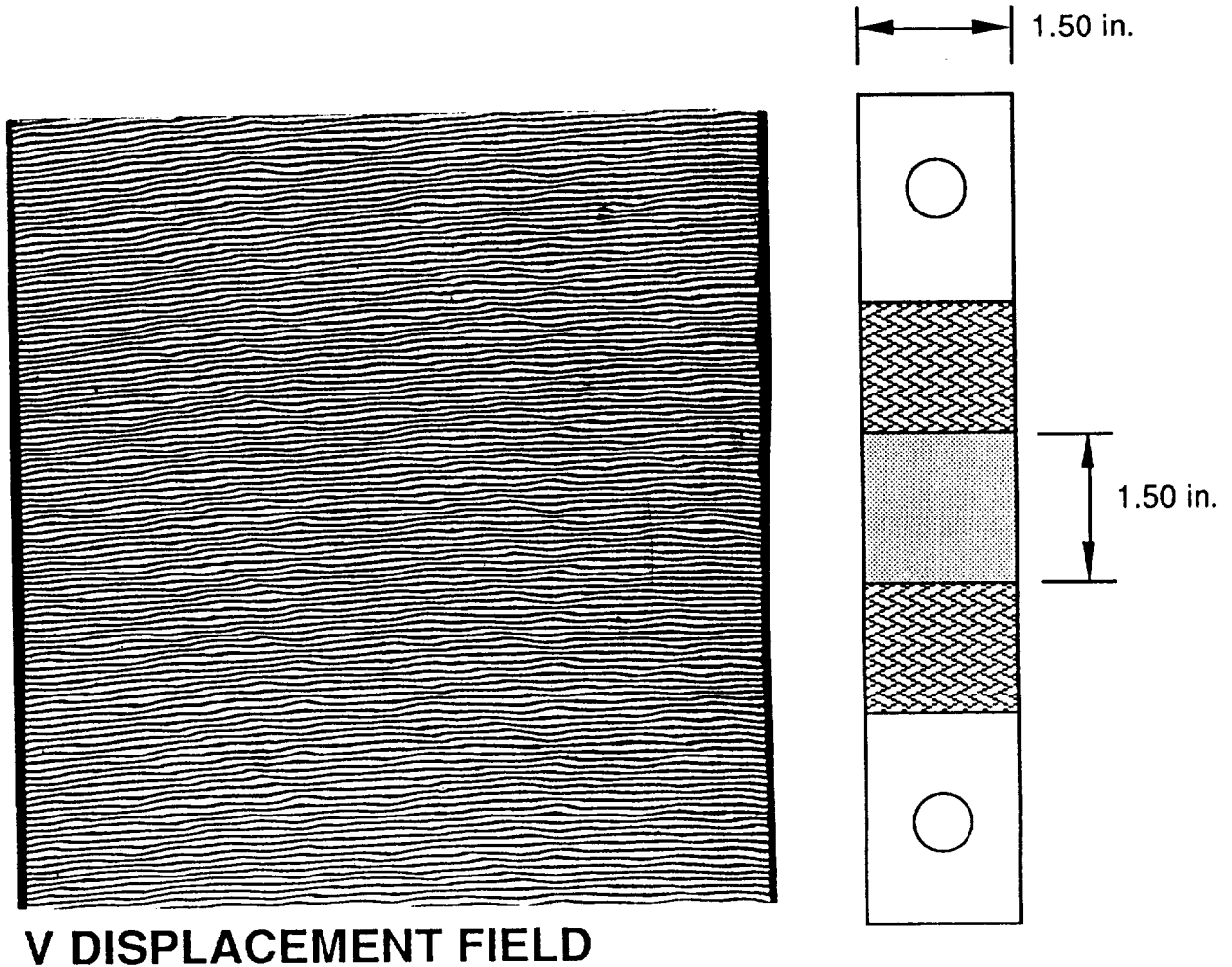
Three preform parameters, braid angle, yarn size, and 0° yarn content, were varied in this study. The last parameter listed is typically expressed as a percentage of 0° yarns. It is the volumetric proportion of longitudinal yarns to total yarn content and is a function of braid angle and yarn size. Yarn size is expressed in terms of the number of filaments per yarn. The AS4 yarns used in these materials have a nominal diameter of 7 microns. The longitudinal yarns were larger than the braided yarns in all cases. The B1 and B2 architectures had the same yarn sizes; they differed in braid angle and 0° yarn content. The preform parameters are listed in the table.

The fabrics were formed with a 144 carrier New England Butt triaxial braider, incorporating 72 longitudinal yarns. The mandrel diameters varied for each architecture. Since the number of carriers was constant, this had the effect of changing the yarn spacing. These parameters are also listed in the table.

The increased 0° yarn content, increased 0° yarn spacing, and decreased braid angle of the B1 architecture compared to the B2 architecture are of note. These factors, cumulatively, may aid in interpreting the experimental results.

MOIRE INTERFEROMETRY

2-D Triaxial Braid - 1200 Microstrain

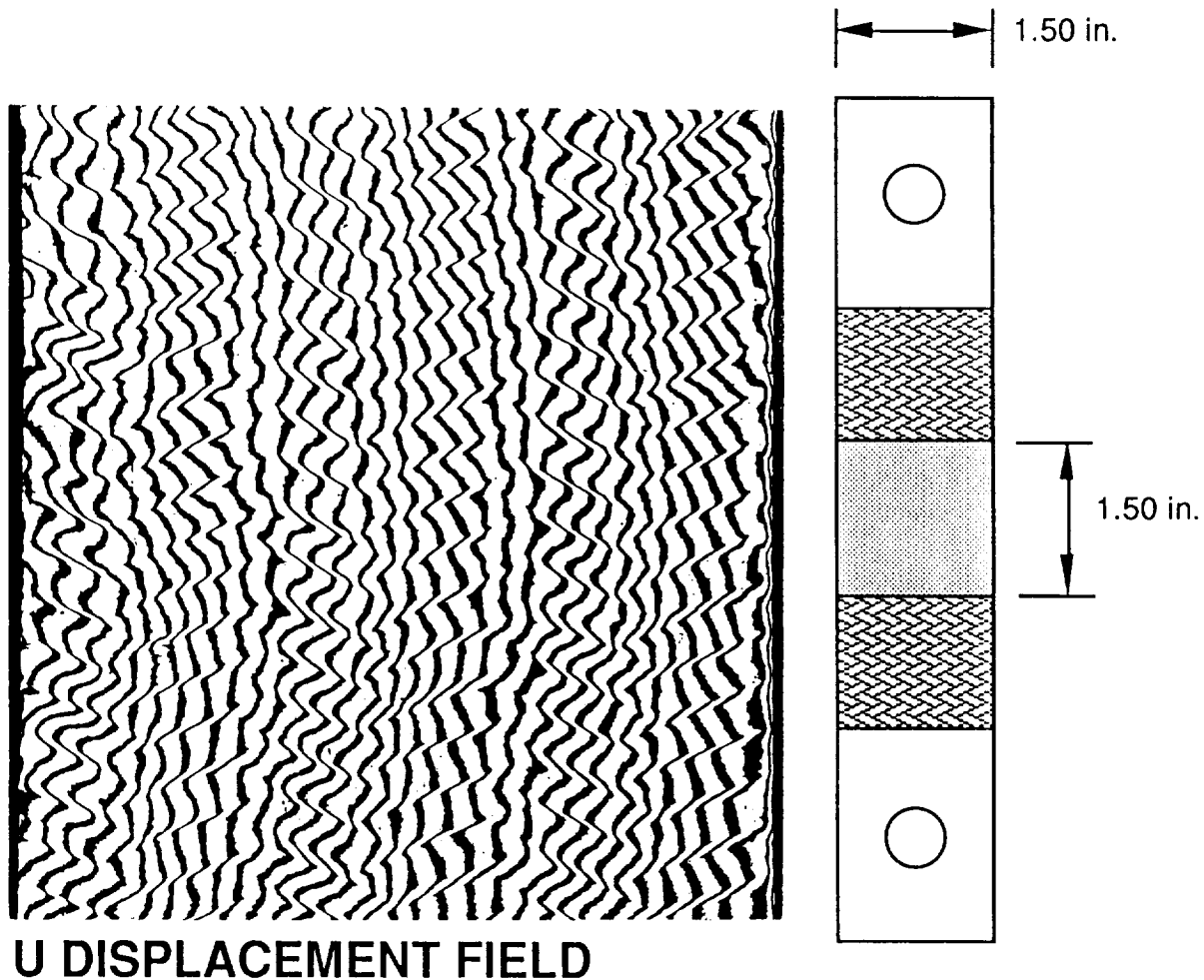


As indicated earlier, Moire interferometry was used to define the full field strain distribution in these braided specimens. The technique defines deformation patterns in both the vertical and horizontal directions. These results are shown in this and the following figure.

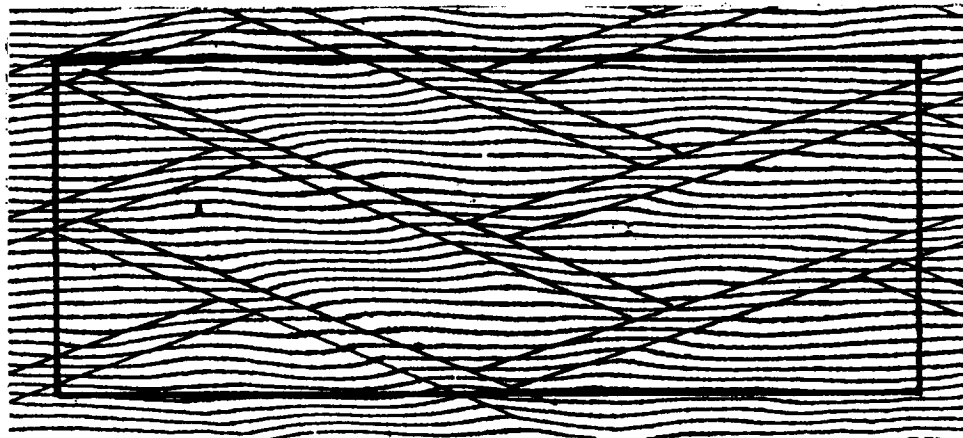
The vertical displacement fields (V fields) consist of basically horizontal fringes; this indicates specimen extension where points along one fringe have been displaced vertically with respect to points along a neighboring fringe. For a uniform extension the fringes should be evenly spaced and straight. The fringes for the specimens tested, however, are wavy and the spacing between them varies. The variation is cyclic and coincides with the repeated unit of the textile architecture.

MOIRE INTERFEROMETRY

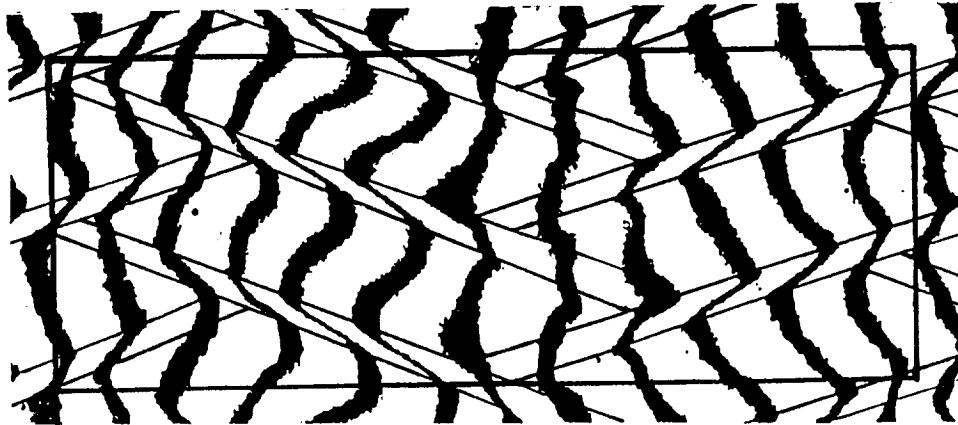
2-D Triaxial Braid - 2400 Microstrain



The horizontal displacement patterns (U fields) consist of zigzag vertical fringes that display the Poisson's effect. For uniform contraction the fringes should be straight and the spacing constant. The fringes, however, display a variation which is cyclic, and matches that of the weave geometry. The sharp kinks in the U field fringes reveal the presence of shear strains between the fiber bundles.



ENLARGED VIEW OF TWO UNIT CELLS - V FIELD



ENLARGED VIEW OF TWO UNIT CELLS - U FIELD

The figure shows the V and U fields of a highly magnified region of specimen that consists of two unit cells. The boundaries between adjacent fiber bundles and the outline of the cells are marked. It was revealed that the shear deformation at interfaces between the fiber bundles occurred over a finite width. This width is illustrated in the patterns as the distance between the closely spaced lines. This is consistent with the presence of the resin rich areas between the fiber bundles, which was on the order of one fifth of the width of the fiber bundle itself. The U field shows that the shear strain γ_{xy} in the resin rich zones was on the order of 0.5 times that of the average applied normal strain ϵ_y . Additionally, the U field shows that the Poisson effect was nearly constant across the unit cell. The V displacement pattern clearly shows that the strain ϵ_y varies significantly within each unit cell as can be seen by the nonuniform fringe spacing. The ratio of maximum strain ϵ_y to minimum strain was about 2.1. The normal strain varies on top of the fiber bundles and is nearly constant throughout all of the resin rich zones.

DAMAGE DEVELOPMENT 2-D TRIAXIAL BRAID (3000 Microstrain)



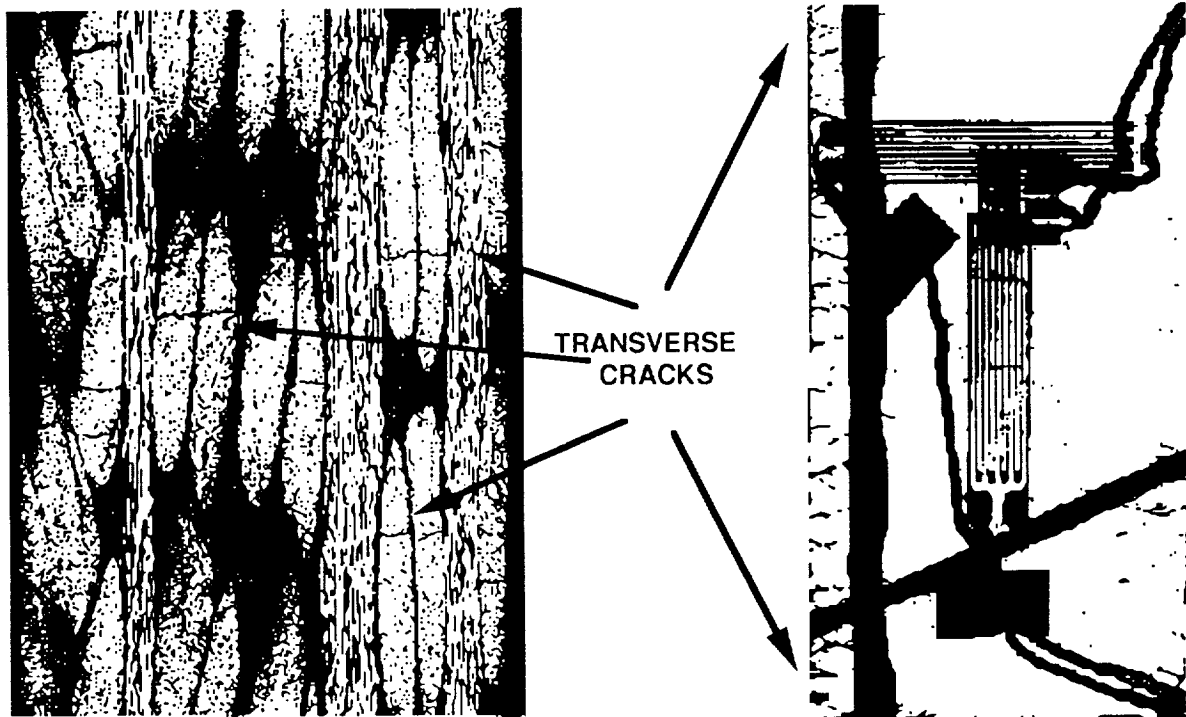
TRANSVERSE CRACKS
- within the braided yarn
bundles

A series of tests were conducted to identify the types and locations of damage that developed in the specimens. The test procedure in these tests was to load the specimens in displacement control while monitoring load and strain. Loading was halted at set strain levels, the specimen was unloaded to a nominal strain level, and inspected. Two nondestructive test techniques, enhanced X-ray radiography and edge replication, were employed. After inspection, the specimen was reloaded to an increased strain level and reinspected. The test continued in this manner until the specimen failed.

Examples of these results are contained in the following figures. They illustrate the damage that developed in B1 specimens under tensile loading in the longitudinal direction.

Damage, in the form of transverse cracks within the braided yarn bundles, was first evident at 3000 - 3500 microstrain. There were very few cracks found at this strain level. They occurred at scattered locations along the specimen length and were evident at the specimen surface only. The crack locations roughly correspond to the regions of high strain identified in the Moire interferometric study.

DAMAGE DEVELOPMENT 2-D TRIAXIAL BRAID (6000 Microstrain)

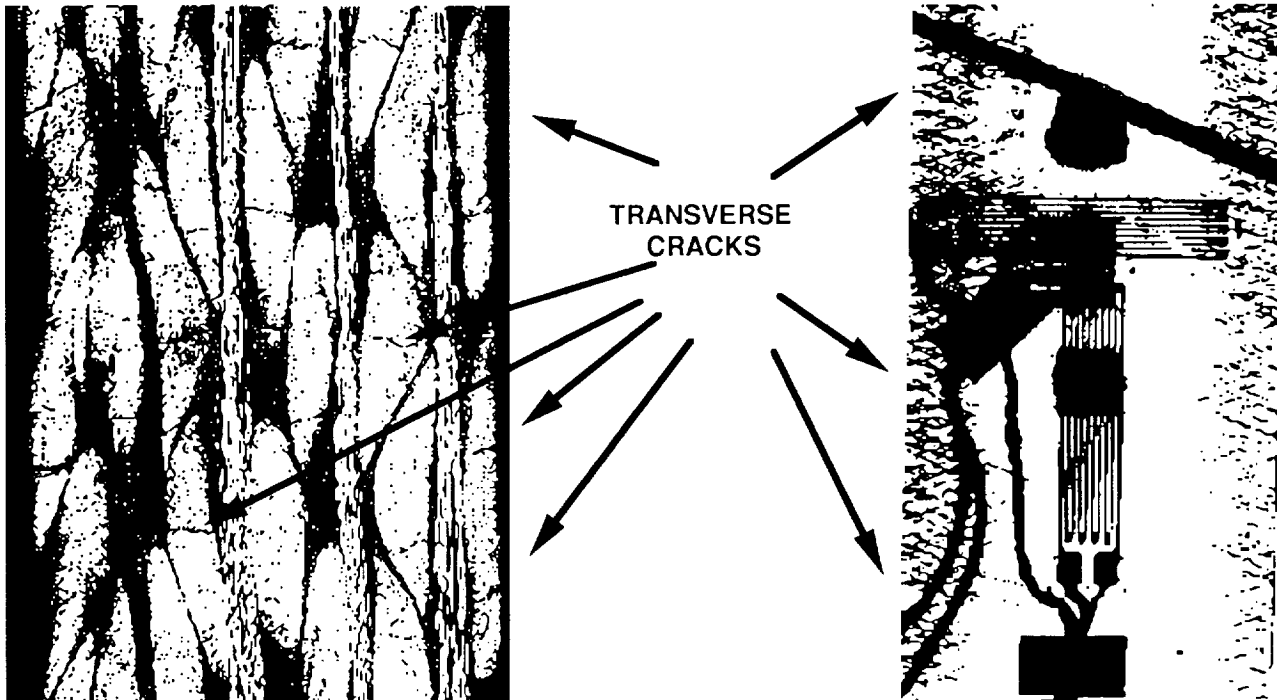


PHOTOMICROGRAPH OF SPECIMEN EDGE

ENHANCED X-RAY OF SPECIMEN FACE

At 6000 microstrain, transverse cracking was evident all along the length of the specimen. This is evident in the enhanced X-ray radiograph shown in this figure. The dark vertical and slanted lines in the radiograph are nickel coated yarn bundles incorporated into the braid to verify yarn orientation. The 1.0 in. long strain gages used on this specimen are also evident in the radiograph. In contrast to the previous figure, the photomicrograph of the specimen edge shown here indicates that damage is evident in the interior of the specimen. Transverse cracks are found in the inner yarn bundles.

DAMAGE DEVELOPMENT 2-D TRIAXIAL BRAID (9500 Microstrain)



PHOTOMICROGRAPH OF SPECIMEN EDGE

ENHANCED X-RAY OF SPECIMEN FACE

Photomicrographs of the edges of the specimen indicate that transverse cracking has increased significantly at 9500 microstrain. Many yarn bundles have sustained multiple transverse cracks. The enhanced X-Ray radiography demonstrates the increased density of the cracks. Even at this advanced load, delamination was rarely evident (none is shown in the figure). When it did occur it developed at the interface of a cracked yarn bundle and the surrounding matrix. These delaminations were limited to a small local regions.

MODULUS AND POISSON'S RATIO TEST RESULTS

MATERIAL	THICKNESS (in.)	FIBER VOLUME (%)	LONGITUDINAL		TRANSVERSE	
			MODULUS (MSI)	POISSON'S RATIO	MODULUS (MSI)	POISSON'S RATIO
A 1	.136	54.0	6.62 ± .22	.300 ± .031	5.64	.264
B 1	.136	48.2	6.55 ± .25	.268 ± .026	-	-
	.127	52.3	7.22 ± .24	.227 ± .007	6.34 ± .09	.214 ± .013
B 2	.138	48.9	6.59	.155	7.12 ± .42	.191 ± .010

The results of the modulus and Poisson's ratio measurements are contained in the table. Strain measurements were made using either 0.500 in. or 1.0 in. long strain gages. The moduli and Poisson's ratios were computed over the 0 to 3000 microstrain region of the stress-strain curves. The slopes of the curves were established through linear regression to the data.

The data in the table indicates that the A1, B1, and B2 architectures had comparable longitudinal moduli. They showed greater sensitivity to architecture when loaded in the transverse direction. As a general observation, the use of strain gages with increased gage length in this study (.500 in. and 1.0 in. vs .062 in., .125 in., and .187 in. used in the previous investigation) reduced the scatter in the data. This was particularly evident in the transverse modulus measurements.

TENSILE STRENGTH TEST RESULTS

MATERIAL	THICKNESS (in.)	FIBER VOLUME (%)	LONGITUDINAL		TRANSVERSE	
			STRENGTH (KSI)	ULTIMATE STRAIN (%)	STRENGTH (KSI)	ULTIMATE STRAIN (%)
A 1	.136	54.0	62.7 ± 3.0	1.06 ± .22	36.1 ± 2.0	0.65 ± .11
B 1	.136	48.2	80.7 ± 1.4	1.36 ± .07	-	-
	.127	52.3	87.3 ± 9.1	1.26 ± .12	41.9 ± 2.5	.70 ± .10
B 2	.138	48.9	57.1 ± 1.6	.95 ± .12	45.0 ± 5.0	.67 ± .12

The tensile strength and ultimate strain measurements are summarized in the table. The data reported show little variation from results reported in a previous evaluation of these materials (NASA Contractor Report 189572, Jan. 1992). Longitudinal strengths and strains were greater than transverse strengths and strains for all three materials. Similarly, the transverse strengths were again comparable for all three materials.

The superior longitudinal strength of the B1 architecture compared to the A1 and B2 materials is again demonstrated in the data. The specimens evaluated in this series of tests had an average fiber volume content of 52.3% and an average tensile strength of 87.3 KSI compared to 48.2% and 80.7 KSI, respectively, in the previous tests. These results confirm observations made in the previous study and again raise the issue of which, if any, braid or material parameter accounts for this dramatic increase in strength over the B2 materials. The two architectures use the same size yarns for both the 0° and braid yarns. However, when laminates of equal fiber volume are compared, the B1 material has a 40% greater longitudinal strength. It may be that the combined effects of the increased 0° yarn content (37.6% vs 34%), the increased 0° yarn spacing (4.77 yarn/in vs 4.37 yarn/in), and the decreased braid angle (66.5° vs 70°) cumulatively account for this discrepancy. This remains a subject of investigation.

5 Modules of Analytical Model

- I. FIBER ARCHITECTURE**
- II. STIFFNESS COMPONENTS OF TEXTILE COMPOSITES**
- III. SHEAR DEFORMABLE PLATE THEORY**
- IV. FAILURE MECHANISMS**
- V. FAILURE PREDICTION**

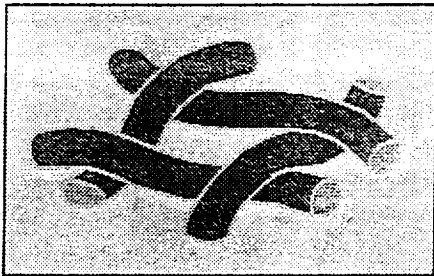
The Textile Composites Analysis (TECA) Model was developed to support Boeing's Advanced Technology Composite Aircraft Structures (ATCAS) Program. In general, TECA predicts the stiffnesses and strengths of textile composites under a variety of loading conditions. The capabilities of TECA have been utilized in a variety of ways during the ATCAS Program. These roles are fiber architecture optimization, parametric studies, material cards for finite element modelling, efficient material characterization, failure mechanism prediction, and insight to potential problem areas. The five modules of TECA are listed below.

Module I: Fiber Architecture Geometry

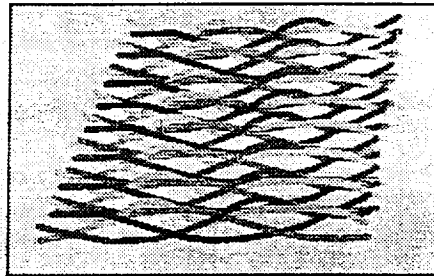
OBJECTIVE: DETAILED PHYSICAL REPRESENTATION OF THE BRAID GEOMETRY

ARCHITECTURE TYPES: 2-D BRAID
2-D TRIAXIAL BRAID
3-D BRAID
WOVEN FABRICS

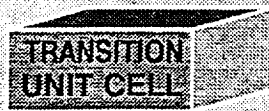
2-D BRAID



3-D BRAID



UNIT CELLS:

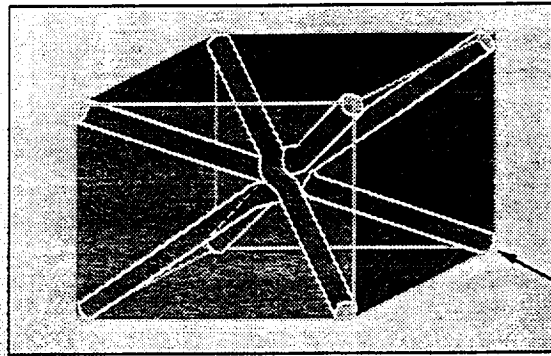


The analysis of textile composite structures requires the knowledge of the internal fiber architecture of the structures. The overall purpose of the Fiber Architecture Geometry Module is to produce a detailed physical representation of the fiber architecture in a braided composite structure. The types of architectures that can be represented by this module include 2-D braids, 2-D triaxial braids, 3-D braids, and woven fabrics.

A handwritten signature or mark, possibly the initials "ed", written in black ink.

Module I: Fiber Architecture

3-D UNIT CELL



ELEMENTAL
COMPONENT
TOW

MODEL INPUT:

- TOW SIZE
- BRAIDING RATIO
- LOOM CONFIGURATION

MODEL OUTPUT:

- DIMENSIONS OF UNIT CELLS
- INTERIOR FIBER ANGLES OF UNIT CELLS
- NUMBER OF UNIT CELLS IN A STRUCTURE

The main assumption contained in the Fiber Architecture Geometry Module is that one can assume that the internal fiber architecture of a braided structure can be represented by a series of repeating building blocks called unit cells. A unit cell is comprised of elemental component tows (an extracted 3-D unit cell from a 3-D braided architecture is shown below). The physical properties of the unit cell are dependent on the manufacturing set-up and the tow characteristics.

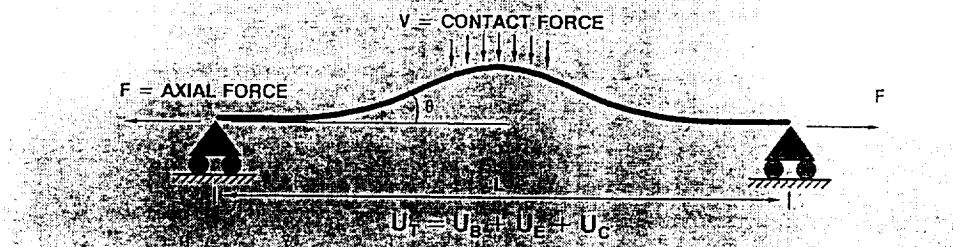
Module II: Global Stiffness of Textile Composites

OBJECTIVE: PREDICT THE EFFECTIVE ELASTIC CONSTANTS OR INELASTIC CONSTITUTIVE RELATIONSHIPS OF TEXTILE PREFORMS FOR STRUCTURAL ANALYSIS

APPROACH:

- CALCULATE THE STIFFNESS MATRIX FOR EACH ELEMENTAL COMPONENT TOW
- TRANSFORM THE ELEMENTAL COMPONENT TOW LOCAL STIFFNESS MATRIX IN SPACE TO FIT THE COMPOSITE AXES
- APPLY A VOLUME AVERAGING APPROACH TO DETERMINE GLOBAL STIFFNESS

Elemental Component Tow Curvature



The overall objective of the Global Stiffness Module is to predict the effective elastic constants or nonlinear constitutive relationships of textile preforms for structural analysis. Non-linear response mechanisms such as shear deformation of the preform, matrix properties, and the effect of matrix cracking are taken into consideration when determining the nonlinear constitutive relationships.

The global stiffness matrix of a braided structure is calculated through the following steps: 1) the stiffness matrix for each elemental component tow is calculated through micromechanics relationships, 2) the local stiffness matrices of the elemental component tows are transformed in space to fit the composite axes, and 3) a volume averaging approach is applied to determine the global stiffnesses.

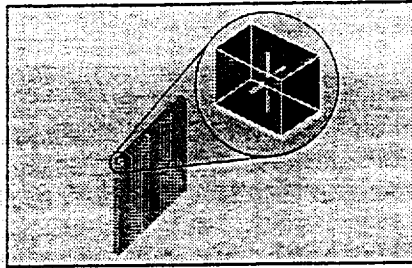
Stiffness modifications were introduced into the model to account for fiber bending because a tow experiences waviness around areas of interlacing and turn-around points as it traverses through a preform. The stiffnesses were modified by an elastic strain energy approach which uses beam elements to represent the bending behavior of a braided tow. The total strain energy includes the strain energy due to bending and extension of the beam elements, and compression in the region of contact in tow cross-over areas.

ORIGINAL PAGE IS
OF POOR QUALITY

ORIGINAL PAGE IS
OF POOR QUALITY

Module III: Stress Analysis

OBJECTIVE: PROVIDE PROPERTIES FOR TRADITIONAL PLATE/SHELL ANALYSIS



APPROACH:

$$1. \begin{bmatrix} C_{11} & C_{12} & C_{13} & C_{14} & C_{15} & C_{16} \\ & C_{22} & C_{23} & C_{24} & C_{25} & C_{26} \\ & & C_{33} & C_{34} & C_{35} & C_{36} \\ & & & E_{11} & E_{15} & E_{16} \\ & & & & E_{44} & E_{45} \\ & & & & & E_{55} \\ & & & & & & C_{66} \end{bmatrix}$$

2. APPLY CONDITION $\sigma_z = 0$

3. INTEGRATE TO OBTAIN EXTENSIONAL AND BENDING STIFFNESS MATRICES

4. ANALYSIS

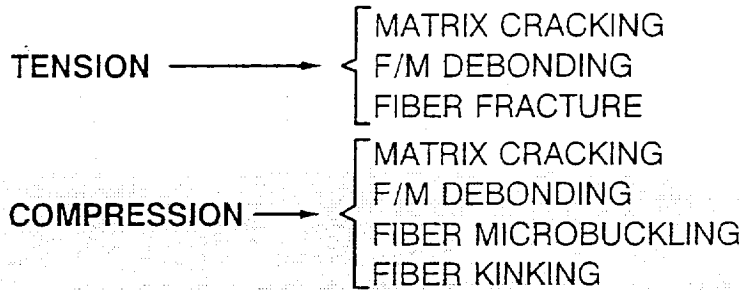
- PLATE ANALYSIS
- SHELL ANALYSIS
- STRESS CONCENTRATION FACTORS

Since most engineering problems are set-up for plate or shell analysis, properties are required in a form compatible with this type of analysis. The third module of TECA performs the necessary analysis utilizing the 3-D stiffness matrix determined in the previous module. First, a plane stress condition is applied (via static condensation) to the 3-D stiffness matrix. Next, integration is performed to obtain the extensional and bending stiffness matrices. Following this step, the stress field in the composite can be calculated using shear-deformable plate analysis or shell analysis.

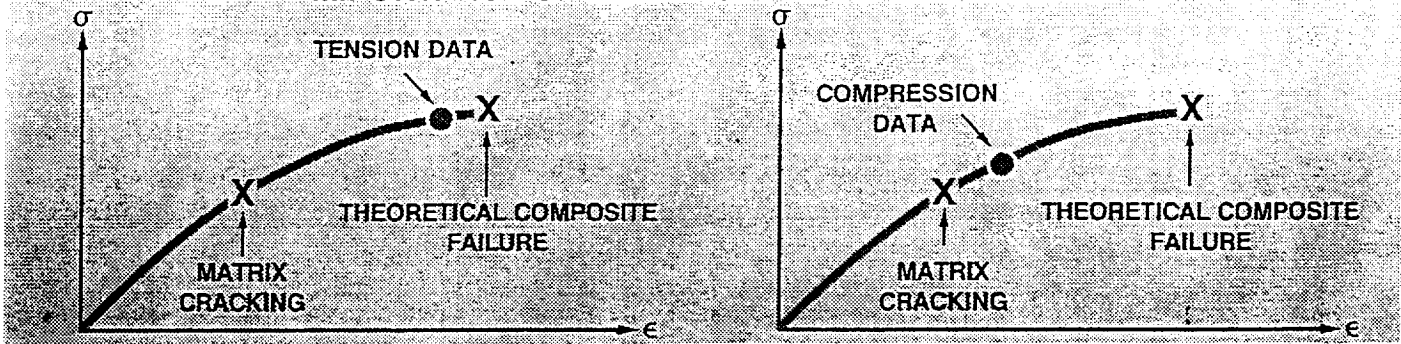
ORIGINAL PAGE IS
OF POOR QUALITY

Module IV: Failure Mechanisms

OBJECTIVE: PREDICT HISTORY OF DAMAGE INITIATION AND FAILURE FOR DIFFERENT TYPES OF LOADING CONDITIONS



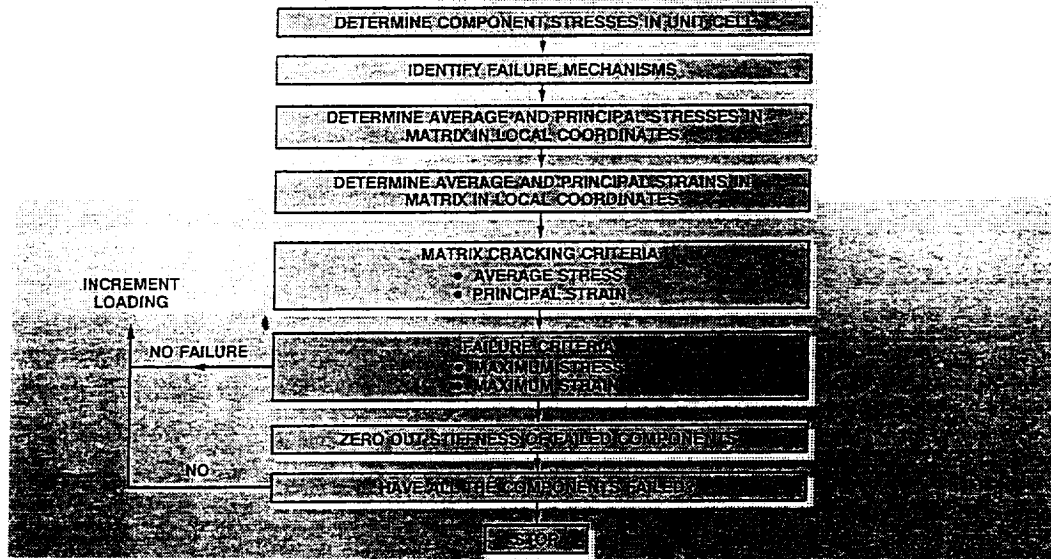
IMPORTANCE OF DEFINING FAILURE MECHANISMS:



In conjunction with the Failure Prediction Module (see next page), the Failure Mechanisms Module identifies the history of failure of textile composites. Specifically, the Failure Mechanisms Module predicts the history of damage initiation and growth to failure for many different types of loading conditions.

ORIGINAL PAGE IS
OF POOR QUALITY

Flow Chart of Failure Prediction



The overall objective of the Failure Prediction Module is to predict the history of failure of a textile composite from average stresses obtained from global structural analysis.

The Strength Module is set-up for a progressive failure analysis using the following sequence of steps: 1) the failure mechanism for the loading condition is identified, 2) the average and principal stresses and strains in the matrix are determined on a local level, 3) the matrix cracking criterion is applied via either an average stress or principal strain criterion (if matrix cracking is detected, the necessary adjustments are made to the local stress field and component stiffnesses), and 4) the failure criteria is applied via either a maximum stress or maximum strain criteria.

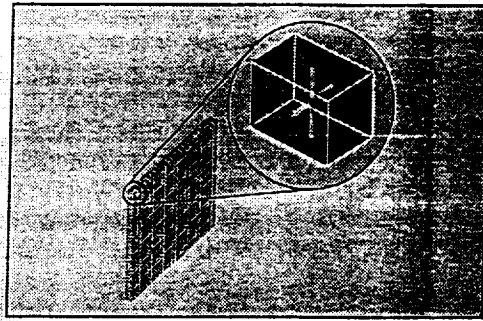
**ORIGINAL PAGE IS
OF POOR QUALITY**

Analysis of Braided Composite Mechanical Behavior

MODEL CAPABILITIES

- UNIT CELL GEOMETRY
 - DIMENSIONS OF UNIT CELL
 - INTERIOR FIBER ANGLES OF UNIT CELL
 - NUMBER OF UNIT CELLS IN A PANEL
- WIDE VARIETY OF LOADING CONDITIONS
 - IN-PLANE TENSION, COMPRESSION, AND SHEAR
 - TRANSVERSE SHEAR
 - BENDING AND TWISTING
 - HYGROTHERMAL
- PREDICTION OF COMPOSITE MODULI AND POISSON'S RATIOS
- PROVIDES MATERIAL CARDS FOR FEM

UNIT CELL

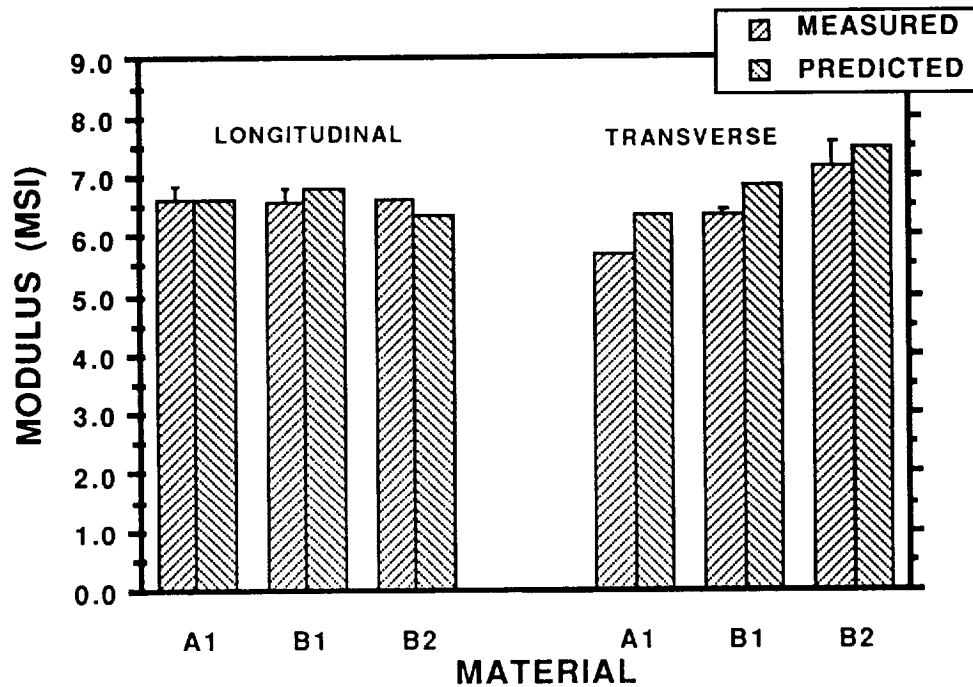


- STRENGTH PREDICTION
 - STRESS STATE WHEN MATRIX CRACKS
 - STRESS AND STRAIN STATE WHEN A COMPONENT FAILS
 - STRESS AND STRAIN STATE OF SUBSEQUENT COMPOSITE FAILURE
 - FAILURE MECHANISM FOR LOAD CASE

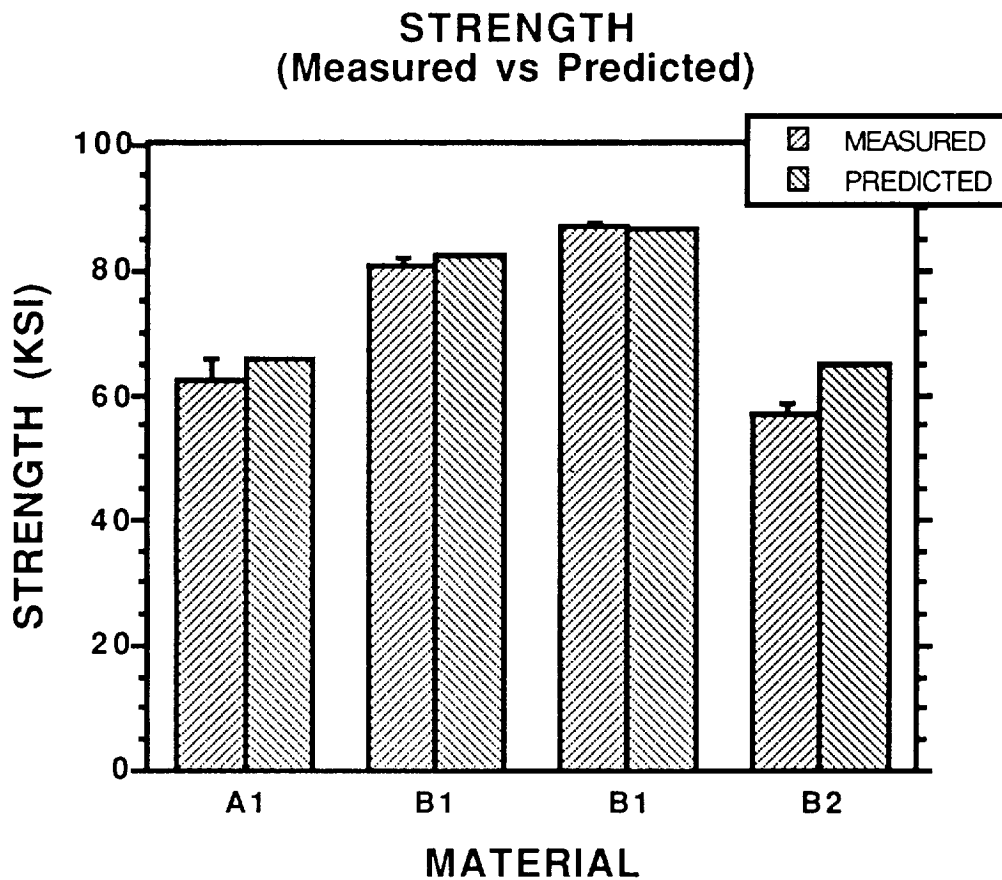
The figure above summarizes the capabilities of the five modules contained in TECA. TECA produces a detailed description of the unit cell geometry for braided composites. The model is capable of performing analysis for a wide variety of loading conditions including in-plane tension, in-plane compression, in-plane and transverse shear, bending, twisting, and hygrothermal loading. The model can predict the composite moduli, composite Poisson's ratios, and composite coefficients of thermal expansion. TECA is also capable of producing material cards for finite element models in which complex shapes can be represented. And finally, the failure criterion contained in TECA can predict the history of failure in a braided composite.

**ORIGINAL PAGE IS
OF POOR QUALITY**

LONGITUDINAL AND TRANSVERSE MODULI (Measured vs Predicted)

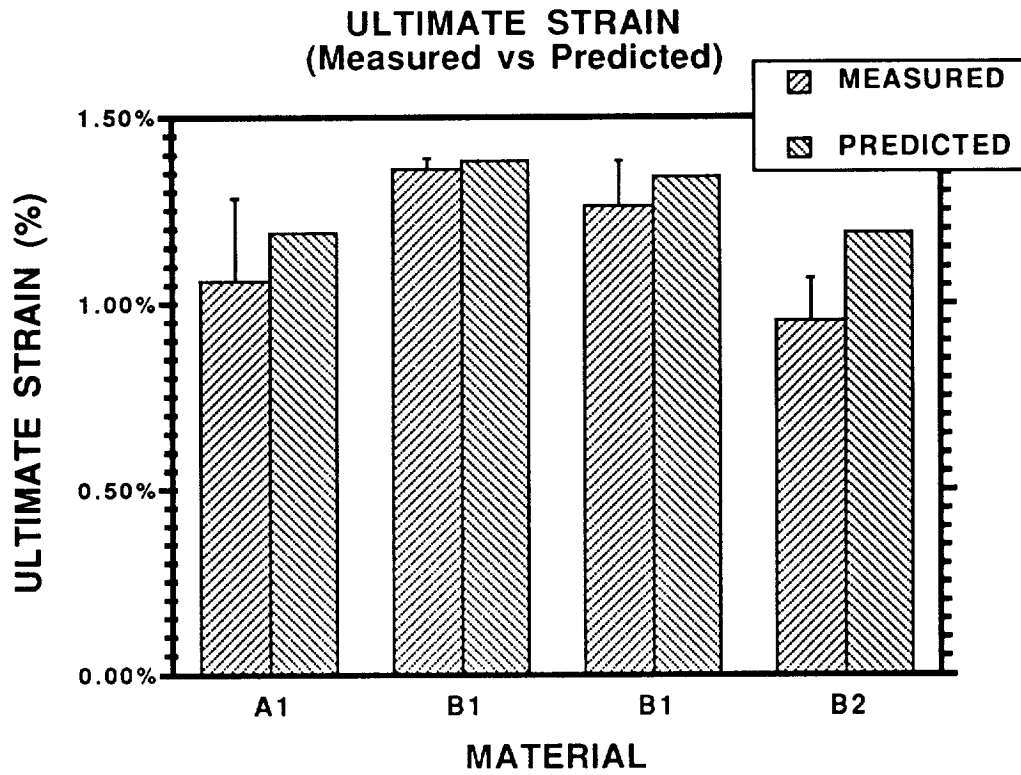


A comparison of the measured and predicted longitudinal and transverse moduli for the three architectures tested is shown in the figure. The data indicate that the values predicted by the TECA model are in close agreement with the experimentally determined values. Previous modelling efforts (NASA Contractor Report 189572) accurately predicted the longitudinal moduli but not the transverse values.



As indicated earlier, an iterative scheme has been incorporated into the TECA model to predict strength and ultimate strain of the braided laminates. The strengths predicted by the model are compared with the experimentally measured values listed previously in this paper. Two strengths are given for the B1 material due to the variation in resin content of the two panels tested.

Although predicted strengths of the A1 and B2 materials were higher than the measured values, the agreement between experimental and analytical values is quite good.



The comparison between measured and predicted ultimate strains for the three architectures is contained in this figure. In general, the model predicted higher strains at failure than were experimentally observed. The predicted values are, however, within the scatter in the data in most cases.

SUMMARY:

- **MEASURED MATERIAL RESPONSE**
- **DEFINED FAILURE MECHANISMS**
- **MOIRE DEFINED DEFORMATION FIELD**
- **MODEL ACCURATELY PREDICTED MECHANICAL RESPONSE**

In summary, the investigation was able to mechanically characterize the mechanical response of the three triaxially braided architectures under tensile loading in both the longitudinal and transverse directions. The materials' moduli and Poisson's ratios were measured along with their strengths. Modulus measurements were improved through the use of .500 in. and 1.0 in. long strain gages but much work is required to develop instrumentation practices for textiles.

The Moire interferometry technique proved to be an effective tool. The definition of the full field strain distribution will be useful both in establishing instrumentation requirements as described in the previous paragraph and in interpreting failure events.

Through the combined use of enhanced X-ray radiography and edge replication, the types and locations of damage were defined. Under this type of loading, damage consists primarily of matrix cracking in the braided yarns. This is first evident at 3000 to 3500 microstrain and continues to develop until failure occurs. Only minor delamination was observed at high strain levels.

The TECA model was effective in modelling both the moduli and strengths of the three architectures. The agreement between measured and predicted longitudinal and transverse moduli were improved compared to previous efforts. The strength predictions also closely agreed with the experimental values.

1